

CRYOLITHOGENESIS

STRUCTURE AND FORMATION CONDITIONS OF THE ICE COMPLEX
IN THE LOWER REACHES OF THE VILYUI RIVER, CENTRAL YAKUTIA

M.R. Pavlova*, A.A. Galanin, V.M. Lytkin, N.V. Torgovkin

*Melnikov Permafrost Institute, Siberian Branch of the Russian Academy of Sciences,
Merzlotnaya St. 36, Yakutsk, 677010 Russia***Corresponding author; e-mail: Nigaer@yandex.ru*

This article presents the results of a comprehensive investigation of the ice complex discovered within the strath terrace in the lower course of the Vilyui River, Central Yakutia. On the basis of chemical, isotopic, granulometric, palynological, and radiocarbon data, it has been revealed that the formation of the ice complex took place from the end of the Kargin (MIS 3) and throughout the Sartan (MIS 2) epochs of the Late Pleistocene (between 29 and 11.7 ka BP) under cryoarid conditions with a predominance of dry cold xerophytic steppes and, locally, forb-grass meadows. Mineralization of syngenetic ice wedges is low ($0.07\text{--}0.29\text{ g/dm}^3$), and a predominance of calcium bicarbonates suggests that winter precipitation – snowmelt water – was the main source of wedge ice. The increased content of heavy metals (Fe, Mn, Co, V, Sr) indicates that the formation of ice wedges also involved the water of shallow freezing lakes confined to the polygonal microrelief. The ice wedges have a relatively light isotopic composition ($\delta^{18}\text{O}$ $-(29.2 \pm 0.3)$ and $-(27.2 \pm 1.4)\text{‰}$; δD $-(226.6 \pm 2.3)$ and $-(215.8 \pm 8.5)\text{‰}$; d_{exc} (6.8 ± 0.51) and $(1.7 \pm 3.1)\text{‰}$), which is close to the composition of modern atmospheric precipitation of the cold season and spring snow storage in Yakutsk. These data attest to dry and cold conditions, thin snow cover, and moisture deficiency in cryogenic landscapes during the formation of the ice complex.

Keywords: *ice complex, ice wedge, chemical composition, isotope analysis, palynology, radiocarbon dating, grain size, Late Pleistocene, Central Yakutia.*

Recommended citation: Pavlova M.R., Galanin A.A., Lytkin V.M., Torgovkin N.V., 2024. Structure and formation conditions of the ice complex in the lower reaches of the Vilyui River, Central Yakutia. *Earth's Cryosphere* XXVIII (6), 3–16.

INTRODUCTION

One of the most striking and constantly debated natural phenomena of northern Eurasia and North America are the covers of syncryogenic ice-rich dispersed sediments with syngenetic ice wedges (IW), referred to as the ice complex (IC) [Romanovsky, 1993]. In the eastern part of the northern Asia, IC sediments are distributed from about 60° N to the Arctic coast [Schirmeister *et al.*, 2022] and represent relicts of cold glacial periods of the Late Pleistocene. A distinctive feature of this type of sediments is a high content of segregated ice and ice wedges, predominantly silty composition, a significant amount of fine-grained (particulate) organic matter, and a large number of the remains of mammoth fauna; IC sediments occur at different hypsometric levels.

One of the centers of the IC distribution is Central Yakutia, where the IC covers as a blanket the surfaces of watersheds and fluvial terraces of the Lena and Vilyui rivers and their tributaries. Generally, IC is found in the form of remnants in the inner parts of dune massifs [Galanin *et al.*, 2019]. The IC in Central Yakutia occurs at 95 to 317 m a.s.l. The maximum thickness (more than 70 m) has been established

within the erosion-accumulative Abalakh Plain (Lena–Amga interfluvium) [Ivanov, 1984]. The Lena–Amga interfluvium is the most studied area of the IC distribution in Central Yakutia. Various issues of the IC structure, distribution, thickness, and paleogeographic conditions have been studied for more than eighty years and have been considered in previous studies [Soloviev, 1959; Katasonov, Ivanov, 1973; Ivanov, 1984]. At the same time, the IC sediments of the Lena–Vilyui interfluvium and the Vilyui River basin as a whole remain insufficiently studied. Some issues of the IC occurrence, structure, and accumulation conditions have been studied within the framework of geological research of the Quaternary sediments of the Vilyui basin [Alekseev, 1961; Giterman, 1963].

Researchers generally agree that IC sediments accumulated as a result of syncryogenic sedimentation and formation of ice wedges in polygonal tundra landscapes of the Late Pleistocene [Schirmeister *et al.*, 2013]. Their accumulation during the interstadial MIS 3 and stadial MIS 2 was favored by the prolonged continental cold climatic conditions with a short warm season of the Late Pleistocene [Schir-

rmeister et al., 2020]. These conclusions were obtained as a result of comprehensive studies of the IC using different methods and approaches in different areas of its distribution, except for the Vilyui River basin. To reconstruct paleoenvironmental conditions of the IC formation in the Vilyui River valley, field works were carried out in the lower course of the river in 2016 and 2021. Two cross-sections of the IC in the upper part of the strath terrace were investigated. The chemical and isotopic composition of ice was analyzed, which allowed us to recognize the hydrochemical settings of the ice formation and accumulation, as well as to assess the paleogeographic conditions. New data were obtained on the structure, particle size, mineralogical and spore-pollen composition, total organic matter content, and the radiocarbon age of the IC sediments.

STUDY SITE

The studied area is located in the southwestern part of the Central Yakutian Lowland within the Vilyui Mesozoic Depression of the Siberian Platform. In the 1960s, M.N. Alekseev [1961] identified six fluvial terraces elevated at 10 to 120 m above the Vilyui River level. The most ancient (lower part of the Middle Pleistocene) formations in the Vilyui River valley include sediments of the sixth (90–120 m above the river) and fifth (70–80 m) terraces. Sediments of the fourth (40–60 m) and third (30–40 m) terraces were assigned to the Middle Pleistocene formations on the basis of findings of fauna of the Tiraspol and Khazar complex [Gromov, 1948; Alekseev et al., 1962; Giterman, 1963]. Alluvial deposits of the second (20–28 m) and first (10–18 m) terraces and synchronous cover loams of lacustrine and deluvial-solifluction origin overlying the high terraces of the Vilyui River are attributed to the Late Pleistocene.

A.A. Galanin [Galanin et al., 2018; Galanin, Pavlova, 2019] studied the Kysyl-Syr outcrop on the right bank of the Vilyui River 20 km downstream from the Kysyl-Syr settlement. According to the classification of M.N. Alekseev [1961], this outcrop is confined to the second terrace of the Vilyui River. The new study concluded that most of the outcrop is composed of eolian medium-grained sands of the Diolkuma Formation (22–24 m thick) dating back to the Sartan epoch (MIS 2); the underlying alluvial sediments (10–12 m thick) were formed 45–30 kyr BP (MIS 3).

The study area is characterized by an extreme continental climate, the mean annual precipitation is 250–300 mm, the mean annual air temperature is –10 to –11°C, and the coefficient of precipitation-to-potential evaporation ratio is 0.7–0.85 [Gavrilova, 1973; Ershov, 1989]. The average thickness of permafrost is 300–400 m, the active layer thickness varies from 0.5 to 2.5 m [Ershov, 1989]. Within the sand massifs (tukulans) of the Vilyui River valley, the active layer thickness is up to 3–5 m [Katasonova, Tolstov, 1963].

Various types of larch forests (bearberry, lingonberry, ledum, moss, sphagnum, and mixed forests) dominate in the vegetation cover of the area. In some places, pine and spruce forests with a mixture of birch are found. Non-forested landscapes represented by meadow, steppe, and semidesert herbaceous communities are fragmentarily developed on floodplains, low terraces, in alas depressions, and on steep slopes [Danilov, 2005]. The IC with syngenetic ice wedges was uncovered within the left-bank 65-m-high strath terrace of the Vilyui River 10 km downstream from the Kysyl-Syr (Fig. 1). The terrace base is composed of Cretaceous sandstone with an apparent thickness of 10 m to 25 m in the low-water period. The Late Pleistocene sedimentary cover of the terrace includes the alluvial member with a thickness of up to 14 m,

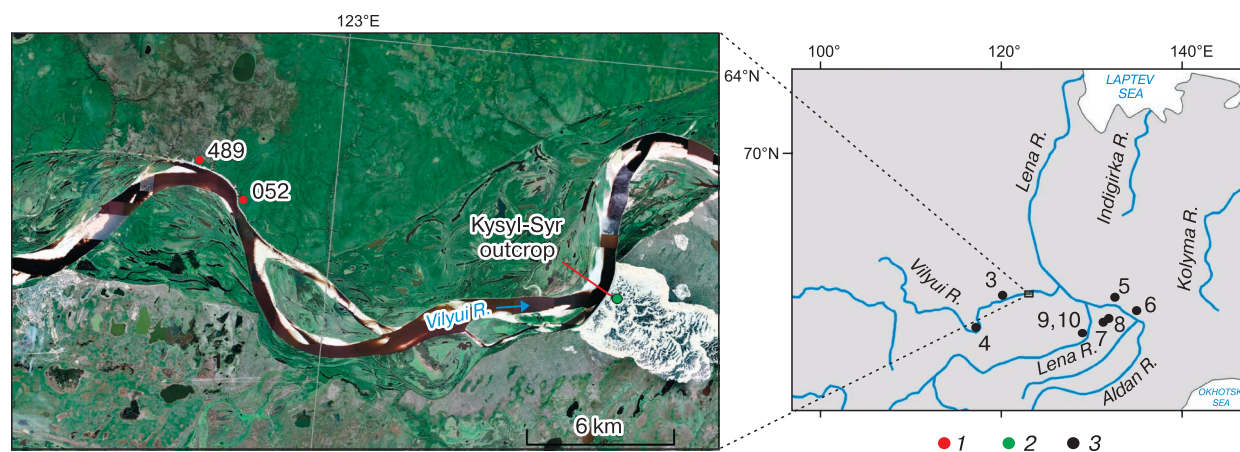


Fig. 1. Geographical location of studied area and key sites.

1 – authors' sections; 2 – Kysyl-Syr outcrop (reference section) [Galanin et al., 2018]; 3 – locations of wedge ice sampling for isotopic analysis (see Fig. 6).



Fig. 2. Strath terrace of the Vilyui River in the lower course, including the ice complex.

a – general view of the terrace (red lines indicate sections 489 and 052); *b* – exposed IC sediments, section 052; *c* – sampling points of ice wedges in section 052 (blue color indicates samples, for which isotopic and chemical analyses were performed).

olian cover sediments of the D'olkuminskaya Series with a thickness of 45–50 m, and the ice complex with a thickness of up to 8 m in the upper part. A more detailed description of the geological structure of the terrace is given in [Pavlova, 2018].

The surface of the terrace is characterized by a hummocky microtopography. Rounded and oval-shaped hummocks are 70–90 cm in diameter and 15–20 cm in height (on average). Ponded water is seen in some hollows between the hummocks. On the terrace surface, there is larch forest with lingonberry–ledum cover.

Two sections (Fig. 2*a,b*) were studied in the upper part of the IC in 2016 (section 489, 63°56'58" N, 122°52'48" E) [Pavlova, 2018; Galanin et al., 2019] and 2021 (section 052, 63°56'15" N, 122°55'14" E). They are located 2.5 km apart within a single 4.5-m-long natural outcrop (Fig. 1). Section 489 is located in the upper part of a retrogressive thaw slump within the terrace body (Fig. 2). The IC was most clearly exposed at this site in 2016. Section 052 was exposed in the summer of 2021 and uncovered the same upper horizon of the IC with the same apparent thickness as in section 489.

MATERIALS AND METHODS

The studied data of this work are based on an integrated study of two sections in the upper part of the IC within the strath terrace of the Vilyui River. Documentation of the IC and sampling of ice and host sediments were performed according to the methodology described in detail in [Hoefs, 1997; Meyer et al., 2002, 2015]. The analytical studies included chemical and isotopic analysis of the ice wedges; particle size, mineralogical, and spore-pollen analyses; determination of organic matter content; and radiocarbon dating of the host sediments. All analyses, except for the determination of the trace element composition of ice, were carried out at the laboratories of the Melnikov Permafrost Institute, Siberian Branch of the Russian Academy of Sciences (Yakutsk).

Particle-size distribution data on the sediments with ice wedges were obtained in accordance with GOST (Russian State Standard) 12536-2014 [2015] using sieve and aerometric methods. The sieve method without water washing with a set of sieves 2, 1, 0.5, 0.25 and 0.1 mm was applied for sandy and sandy loam samples; clayey sediments were analyzed

by the aerometric method. A total of 22 samples were analyzed for sections nos. 489 and 052.

Quantitative mineralogical analysis of samples from section 489 (two samples from the IC sediments, and two samples from the underlying sediments of the Diolkuma Formation) was performed by the immersion method using binocular and polarizing microscopes and immersion liquids [Sakharova, Cherkasov, 1970]. Minerals were counted for the fraction of 100–250 μm . In each sample, 300–350 grains were counted from a random sample, on the basis of which the percentages for each mineral were calculated.

Radiocarbon analysis (one sample from section 052) was performed by liquid scintillation of plant remains. Calibration of ^{14}C -dates was performed using OxCal 4.4 program [Bronk, 2009] and IntCal 20 calibration curve [Reimer et al., 2020] for 95% significance level with calculation of an average value. The dates for section 489 were obtained by the authors earlier [Shaposhnikov et al., 2019].

Spore-pollen analysis. For the host sediments of the 65-m terrace (section 489), chemical processing of 12 samples was carried out using an adapted technique based on the methods of V.P. Grichuk [Pokrovskaya, 1950] and Faegri–Iversen [Faegri, Iversen, 1989]. Microscopy was performed using a Zeiss PRIMO STAR transmitted light microscope at 400x magnification. At least 300 pollen grains were counted; spores and non-pollen palynomorphs were also documented. Pollen grain concentrations were calculated and spore-pollen diagrams were constructed using the TILIA 2.0.41 program [Grimm, 2004]. Pollen and spore percentages were calculated from the total of all determined pollen grains and spores.

Total organic matter (I_T) was determined for section 489 (12 samples). The loss on ignition in a muffle furnace at 450°C was determined in the air-dried samples of 10–20 g according to GOST 23740-2016 [2017].

Chemical analysis. Ice wedges were sampled along a horizontal profile at a depth of 2.4 m from the terrace surface. Physical and chemical parameters and major ions (052 – three samples, 489 – two samples) were determined by titrimetric and capillary electrophoresis methods. The total mineralization was characterized according to the classification of S.L. Shvartsev [1996]. The Na/Cl metamorphization coefficient of water was calculated according to the method of V.A. Sulin [Alekin, 1975].

The trace element composition was studied by the ICP-MS and ICP-AES methods at the Analytical Certified Testing Center of the Institute of Microelectronics Technology Problems and Highly Pure Materials, Russian Academy of Sciences, Chernogolovka. The concentrations of trace elements were determined for 16 wedge ice samples from section 052 (Fig. 2c). To identify geochemical differences, the

concentrations of trace elements in the wedge ice were compared and normalized to natural abundances of these elements in river water [Solovov et al., 1990], because the mineralization of wedge ice was small and comparable to that of river water.

Isotopic analysis. The isotopic composition ($\delta^{18}\text{O}$, δD) of ice wedges was determined for 16 samples from section 052 (Fig. 2c) by laser absorption infrared spectrometry on a Picarro L2140i analyzer. Water and snow samples calibrated relative to the International Standard V-SMOW-2 (IAEA) were used as internal standards. Statistical processing of the results included the calculation of deuterium excess (d_{exc}) and basic statistical characteristics by standard methods, as well as the plotting in $\delta^{18}\text{O}/\delta\text{D}$ coordinates, and the comparison with the data of the global meteoric water line (GMWL). To identify geochemical and isotopic differences and similarities of the wedge ice, comparisons were made with modern surface and ground waters of the study region, as well as with atmospheric precipitation sampled in different periods of the year. The results of the isotopic analysis of ice for section 489 have been obtained by the authors earlier and are given in [Galanin et al., 2019].

RESULTS

As a result of field observations, we identified and documented the IC sediments in the upper part of the strath terrace in the lower reaches of the Vilyui River in the interval of 0–5 m, in some places up to 8–10 m from the terrace surface.

The IC sediments exposed in sections 489 and 052 have the following structure (from top to bottom) (Fig. 3):

0–0.1 m – Litter layer.

0.1–1.4(2) m – cover sediments represented by brown sandy loams with an interlayer enriched in charcoal. The active layer boundary is traced at a depth of 1.4(2) m and corresponds to the upper boundary of the IC.

Two members are identified below. The first one lies in the interval of 1.4–4.0 m and consists of alternating sandy loam and loamy sands with interlayers of heavy silty sand loams with banded cryogenic fabric. The sediments are heavily saturated with organic detritus and roots of herbaceous plants and contain inclusions of small wood fragments. The water moisture content decreases from 38% at the top to 10.5% at the bottom of this member.

The second member (4.0–4.7 m) is represented by dark brown silty sands with banded cryogenic fabric. The bands are 3- to 5-cm-thick, the distance between them is 5–8 cm and gradually decreases upward along the section. The sediments are saturated with organic detritus with inclusions of woody fragments. The water content is 33.9–35.2%. The lower boundary is distinct, wavy and is marked by the transition from dark to light color of sediments.

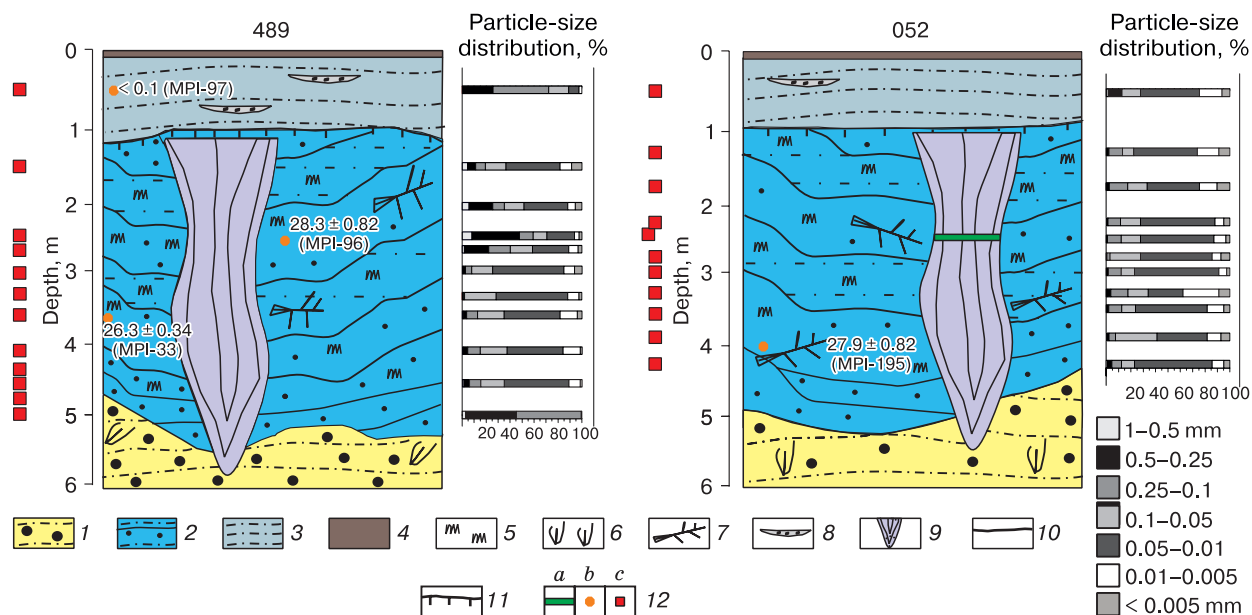


Fig. 3. Schematic structure of the ice complex in sections 489 and 052 within the upper part of strath terrace.

1 – interlayering of light gray medium-grained sands, slightly wavy and slightly inclined parallel-layered, and silty loamy sands (Diolkuma Formation); 2 – alternation of light brown and dark brown silty loamy sands and silty sands with banded cryogenic structures (ice complex sediments); 3 – brown silty loamy sands with charcoal interlayers (Late Holocene cover sediments); 4 – soil litter layer; 5 – organic detritus and inclusions of shrubby vegetation remains; 6 – dead vertically buried stems and clumps of grasses; 7 – horizontally buried fossil trees; 8 – charcoal interlayers; 9 – syngenetic ice wedges; 10 – roof of cover sandy sediments of the Diolkuma Formation; 11 – permafrost table; 12 – sampling point for (a) isotopic and chemical, (b) radiocarbon, and (c) particle-size distribution and spore-pollen analyses.

4.7–5.0 m and deeper – light gray silty sand with admixture of organic detritus, with ocherous mottles and inclusions; dry permafrost; this is a transitional member from the IC sediments to the Diolkuma Formation.

5(8)–51 m – sediments of the Diolkuma Formation – light gray medium-grained quartz sands, slightly wavy, slightly inclined, with parallel layering, of 0.2–0.4 to 8–10 m in thickness alternating with loamy sands of coarser grain size (0.1–0.4 mm). The water content does not exceed 5%.

The mineral composition of the IC sediments, according to the classification of P.I. Fadeev, is quartz-feldspathic (the quartz content does not exceed 88.2%).

Syngenetic ice wedges penetrating the IC reach a width of 2–3 m at the top and form a polygonal network with a cross-section of about 10–12 m; in some places, ice wedges penetrate into the underlying sandy sediments of the Diolkuma Formation to a depth of 1–3 m.

Radiocarbon dating. The results are presented in Table 1.

Table 1. Results of radiocarbon dating of organic material from sediments of the IC on strath terrace of the Vilyui River in its lower course

Laboratory number	Section No.	Sampling depth, m	Material	Age ^{14}C , BP	Calendar age*, cal BP	Source
MPI-97	489	0.5	Charcoal	<100	–	[Shaposhnikov et al., 2019]
MPI-96	489	2.5	Remains of shrub vegetation	23 970 ± 800	28 370 ± 820	Same
MPI-33	489	3.5	Humus from humified loamy sand	22 000 ± 300	26 350 ± 340	Same
MPI-195	052	4.0	Remains of woody vegetation	23 630 ± 550	27 980 ± 560	Authors' data

*Significance level $p > 94.5\%$.

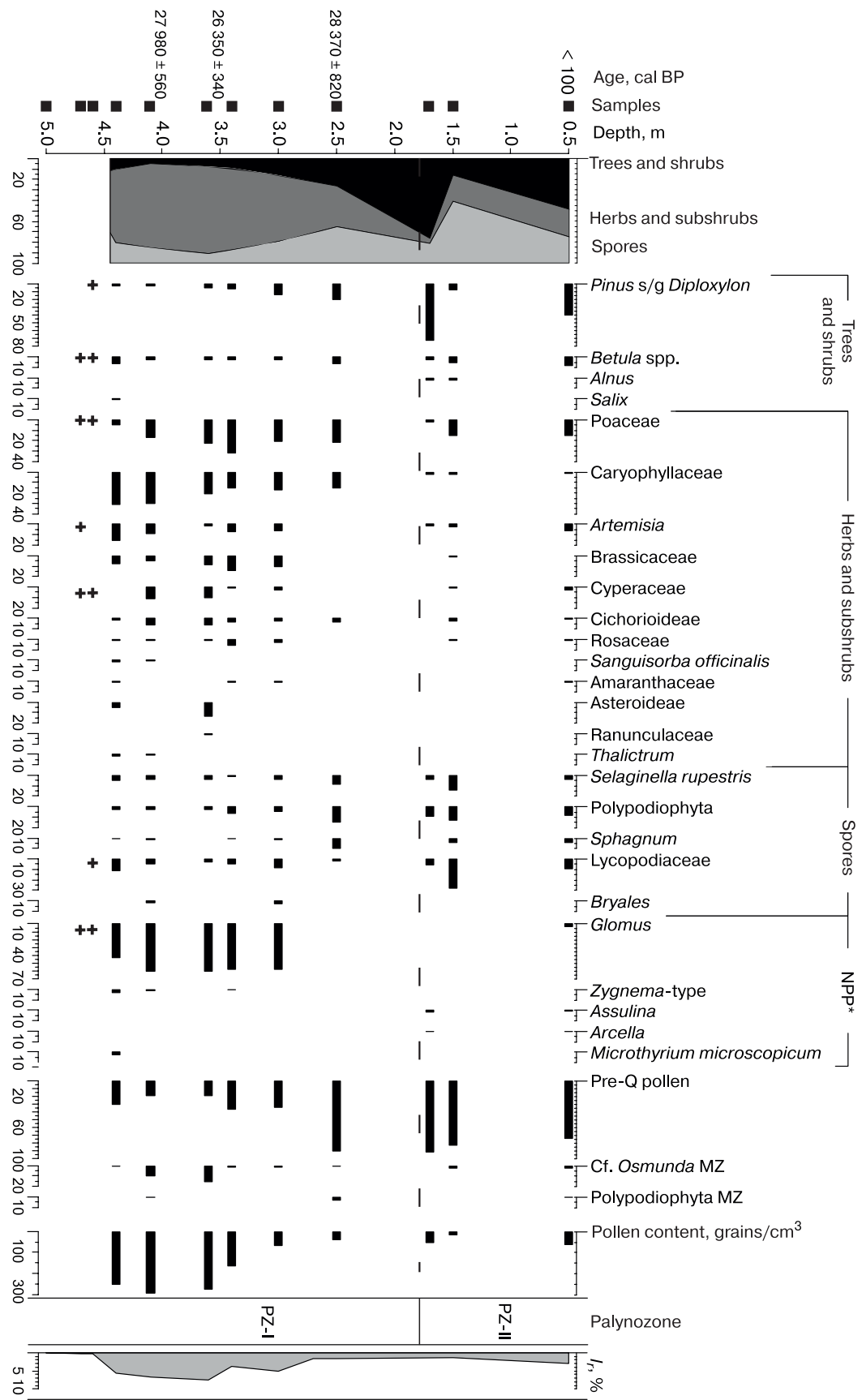


Fig. 4. Palynological diagram and organic matter content (I_r) of section 489 of the ice complex sediments on strath terrace of the Vilyui River in its lower course.

* NPP – non-pollen palynomorphs.

Table 2. Chemical composition and metamorphization coefficient of ice wedges sampled in the upper part of strath terrace of the Vilyui River in its lower course, Central Yakutia

Sample number	pH	Eh	units	Concentration of major cations and anions										Hardness	Mineralization, g/dm ³	Chemical composition according to [Shwartssev, 1996]	Na/Cl
				Ca ²⁺	Mg ²⁺	Na ⁺	K ⁺	NH ₄ ⁺	HCO ₃ ⁻	Cl ⁻	SO ₄ ²⁻	NO ₂ ⁻	NO ₃ ⁻				
052-1	6.32	391	mg/L	48.77	14.80	4.2	1.0	0.05	195.85	12.6	3.55	0.06	10.0	0.29	HCO ₃ 86	0.33	
			meq/L	2.43	1.22	0.18	0.03	0.00	3.21	0.26	0.10	0.00	0.16	3.650	Ca 63 Mg 32		
			mg/L	28.51	10.59	3.3	0.90	0.10	136.26	6.5	2.37	0.02	2.75	0.19	HCO ₃ 90		
052-15	6.41	384	meq/L	1.42	0.87	0.14	0.02	0.004	2.23	0.14	0.07	0.00	0.04	2.293	Ca 58 Mg 35	0.51	
			mg/L	17.26	9.56	1.8	0.7	0.05	88.97	8.0	2.37	0.03	0.11	0.13	HCO ₃ 86		
052-23	6.51	390	meq/L	0.86	0.79	0.08	0.02	0.004	1.46	0.17	0.07	0.001	0.002	1.647	Ca 49 Mg 45	0.23	
489-1	7.54	482	mg/L	25.17	9.16	2.6	1.3	0.06	111.13	6.58	2.78	0.01	7.8	0.17	HCO ₃ 84	0.40	
			meq/L	1.26	0.75	0.11	0.03	0.004	1.82	0.14	0.08	0.002	0.126	2.010	Ca 58 Mg 35		
489-5	6.61	513	mg/L	10.06	3.82	1.6	0.8	1.4	44.95	3.46	3.48	3.0	1.6	0.07	HCO ₃ 74	0.46	
			meq/L	0.50	0.31	0.07	0.02	0.1	0.74	0.07	0.10	0.065	0.026	0.816	Ca 50 Mg 31		

Wedge ice, sampled in 2021 (section 052)

Wedge ice, sampled in 2016 (section 489)

Note: pH – hydrogen index; Eh – redox potential.

Palynological analysis. According to the results of palynological analysis, two palynozones were identified for section 489 (Fig. 4):

Palynozone PZI (interval 4.7–1.8 m) is characterized by the dominance of pollen from herbaceous communities (39.3–82.9%) with a predominance of families Poaceae (4.6–31.7%), Caryophyllaceae (4.6–31.2%), Brassicaceae (5.3–13.8%), and species *Artemisia* (1.6–15.4%) together with *Glomus* spores (42.8 to 60.5%). Pollen of Amaranthaceae, Cichorioideae, Asteroideae, Cyperaceae, Rosaceae (Rosaceae gen sp., *Sanguisorba officinalis*), and Ranunculaceae (Ranunculaceae gen sp., *Thalictrum*) families and subfamilies is also present. In the woody group (5.3–26.2%), pollen of *Pinus* s/g *Diploxylon* (from 2.6 to 19.7%), birch *Betula* spp. (2.4–6.6%), and single grains of willow *Salix* are noted. The sum of spores is 8.9–34.4%; spores of Lycopodiaceae (1.6–11.2%), *Selaginella rupestris* (1.2–8.2%), and Polypodiophyta (2.4–14.8%), *Sphagnum* (0.6–9.8%), and *Bryales* (1.5–2.4%) mosses predominate. Pollen of pre-Quaternary Pinaceae and Podocarpaceae comprise 18.5–89.4% of the total count of all pollen grains, spores, and non-pollen palynomorphs; pre-Quaternary spores of Polypodiophyta and Cf. *Osmunda* and non-pollen palynomorphs – *Microthyrium microscopicum*, *Gelasinospora*, and *Zygnema*-type – have also been identified. Pollen concentration is 39–293 grains/cm³.

Palynozone PZII (interval 1.8–0.5 m) is characterized by a sharp decrease in the pollen of herbs (4.9–26.6%) and an almost complete absence of *Glomus* spores (0–3.5%). The pollen of a group of trees and shrubs accounts for up to 76.5%. Pollen of *Pinus* s/g *Diploxylon* (8–71.6%), *Betula* spp. (2.9–8.5%), and *Alnus* (2–2.3%) is present in the spectra. The herbaceous group is dominated by Poaceae (2–14.9%), *Artemisia* (1.0–6.2%), and Caryophyllaceae (1.1–2.3%). The families Cichorioideae, Rosaceae, Cyperaceae, Brassicaceae and Amaranthaceae have also been identified. The sum of spores is 18.6–58.6%, including *Selaginella rupestris* (3.4–13.8%), Polypodiophyta (8.5–12.6%), *Sphagnum* (4.0–4.6%), Lycopodiaceae (15.9–27.6%). Pre-Quaternary pollen (73.5–90.2%) is mainly represented by the pollen of Pinaceae and Podocarpaceae; there are also pre-Quaternary spores of Polypodiophyta and Cf. *Osmunda* and shells of testate amoebae *Assulina* and *Arcella*. Pollen concentration is 12–59 grains/cm³.

Determination of the total organic matter content. Figure 4 demonstrates the results of the total organic matter (I_r) determination for section 489. In the interval 5.0–4.4 m, the value of I_r is low and gradually increases from bottom to top from 0.14 to 0.35%. In the middle part of the section (4.4–2.7 m), where the sediments are highly enriched in organic detritus, the I_r content is 3.89–7.59%. In the interval of 2.7–0.5 m, the I_r decrease to 1.36–1.63%. At a depth of 0.5 m, in modern sediments (age MPI-97, <100 years) the I_r value increases again to 2.97%.

Table 3. Concentrations of trace elements in wedge ice sampled in the upper part of strath terrace of the Vilyui River in its lower course in 2021 (section 052)

Element	Element concentration, µg/L			Element	Element concentration, µg/L		
	min.*	max.**	mean*** (n = 16)		min.*	max.**	mean*** (n = 16)
B	3.2	7	4.9	Sn	0.031	0.053	0.027
Al	295	1165	534.3	Sb	0.042	0.072	0.049
Ti	8.6	20.8	14.0	Cs	0.012	0.033	0.018
V	2.7	7.5	4.3	La	0.457	2.774	1.096
Cr	1.1	2.2	1.3	Ce	0.965	6.338	2.332
Mn	6.7	106	34.1	Pr	0.130	0.703	0.272
Fe	517	6628	1650.6	Nd	0.503	2.873	1.124
Co	0.22	1.4	0.6	Sm	0.112	0.567	0.224
Ni	2	5.2	3.1	Eu	0.022	0.129	0.048
Cu	3.1	6.7	5.0	Gd	0.101	0.559	0.219
Zn	0.87	6.8	2.7	Tb	0.015	0.083	0.033
As	0.11	0.71	0.3	Dy	0.083	0.432	0.171
Br	22.7	51	29.5	Ho	0.017	0.081	0.033
Sr	52.5	128	77.3	Er	0.044	0.226	0.092
Ba	20.3	76	34.9	Tm	0.060	0.031	0.013
Pb	0.2	1.6	0.6	Yb	0.042	0.191	0.080
Li	0.903	2.025	1.361	Lu	0.060	0.028	0.012
Be	0.025	0.164	0.056	Hf	0.030	0.094	0.043
Rb	0.320	0.669	0.445	Ta	0.006	0.019	0.015
Y	0.429	2.369	0.909	W	0.005	0.011	0.007
Zr	1.270	3.249	1.624	Tl	0.004	0.007	0.005
Nb	0.029	0.058	0.042	Bi	0.003	0.014	0.005
Mo	0.233	0.517	0.328	Th	0.062	0.193	0.114
Ag	0.007	0.727	0.098	U	0.111	1.169	0.382
Cd	0.006	0.024	0.009				

* min. – minimum value;

** max. – maximum value;

*** mean – average value.

Hydrochemical analysis. Based on the analysis of the obtained data, it was established (Table 2) that ice is moderately fresh (mineralization is 0.07–0.29 g/dm³), of magnesium–calcium bicarbonate composition. According to the classification of O.A. Alekin [1975], the samples collected from the marginal part of the ice wedge (nos. 052-1 and 489-1) belong to the third type ($\text{Ca}^{2+} + \text{Mg}^{2+} > \text{HCO}_3^- +$

SO_4^{2-}); samples from the middle part (nos. 052-15, 052-23, 489-5), belong to the second type ($\text{HCO}_3^- < \text{Ca}^{2+} + \text{Mg}^{2+} < \text{HCO}_3^- + \text{SO}_4^{2-}$). This composition and the ratio between the main ions are typical of the continental type of salinity. The coefficient of metamorphization (Na/Cl) in all the studied ice samples is less than 1, which indicates that wedge ice formed from waters of different degrees of metamorphization.

Table 4. Isotopic composition of syngenetic ice wedges sampled in the upper part of strath terrace of the Vilyui River in its lower course

Section no.	Year of sampling	Age	n	$\delta^{18}\text{O}_{\text{min}}$, ‰	$\delta^{18}\text{O}_{\text{max}}$, ‰	$\delta^{18}\text{O} + \text{St. Dev.}$, ‰	$\delta\text{D}_{\text{min}}$, ‰	$\delta\text{D}_{\text{max}}$, ‰	$\delta\text{D} + \text{St. Dev.}$, ‰	$d_{\text{exc min}}$, ‰	$d_{\text{exc max}}$, ‰	$d_{\text{exc}} + \text{St. Dev.}$, ‰
052	2021	MIS 3–2	16	–30.0	–28.6	-29.2 ± 0.3	–231.9	–221.8	-226.6 ± 2.3	6.1	8.5	6.8 ± 0.5
489	2016*	MIS 2	6	–27.6	–24.3	-27.2 ± 1.4	–218.3	–198.7	-215.8 ± 8.5	–4.5	2.5	1.7 ± 3.1

Note. $\delta^{18}\text{O}_{\text{min}}$ – minimum value of stable oxygen isotope, $\delta^{18}\text{O}_{\text{max}}$ – maximum value of stable oxygen isotope, $\delta^{18}\text{O} + \text{St. Dev.}$ – average value of stable oxygen isotope and standard deviation, $\delta\text{D}_{\text{min}}$ – minimum value of stable hydrogen (deuterium) isotope, $\delta\text{D}_{\text{max}}$ – maximum value of stable hydrogen (deuterium) isotope, $\delta\text{D} + \text{St. Dev.}$ – average value of stable hydrogen (deuterium) isotope and standard deviation, $d_{\text{exc min}}$ – minimum value of d-excess, $d_{\text{exc max}}$ – maximum value of d-excess, $d_{\text{exc}} + \text{St. Dev.}$ – average value of d-excess and standard deviation.

* According to [Galanin et al., 2019].

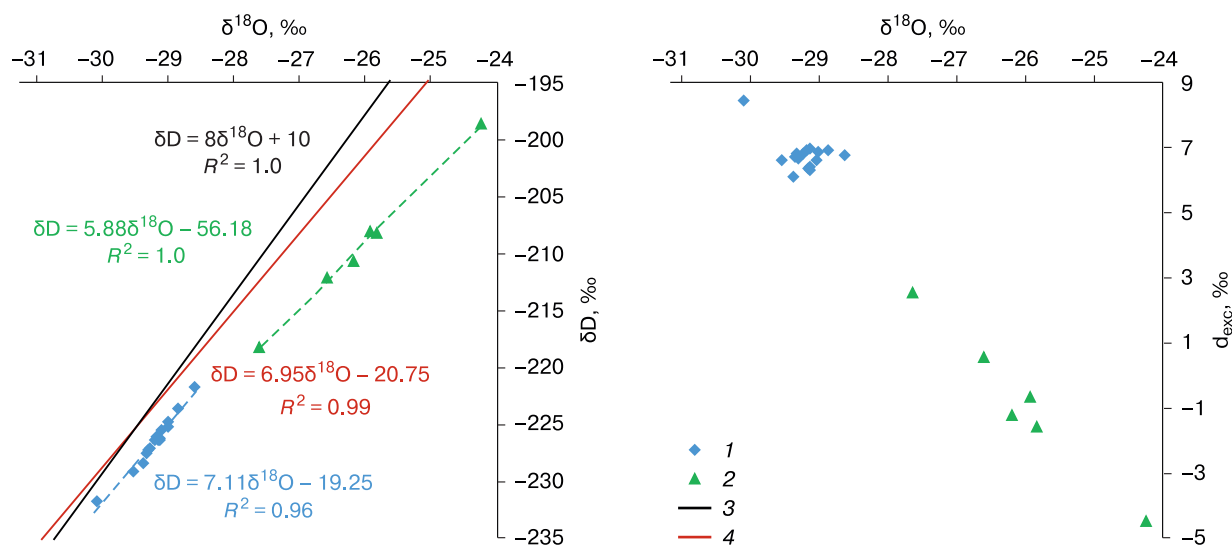


Fig. 5. Isotopic composition values $\delta^{18}\text{O}/\delta\text{D}$ and $\delta^{18}\text{O}/d_{\text{exc}}$ and regression equations for ice wedges on strath terrace of the Vilyui River in its lower course.

1 – samples collected in 2021; 2 – samples collected in 2016; 3 – global meteoric water line (GMWL); 4 – local meteoric water line (LMWL) [Papina et al., 2017].

Trace element composition. Ice wedges are characterized by the presence of a rather wide range of trace elements (49) (Table 3). The highest concentrations in the ice samples was noted for the following elements (average value for 16 samples, $\mu\text{g}/\text{L}$): Fe (1650.6), Al (534.3), Sr (77.3), Ba (34.9), Mn (34.1), Br (29.5), Ti (14.0), Cu (5.0), B (4.9), V (4.3), Ni (3.1).

Isotopic analysis. The results of the isotopic composition of the ice wedges are presented in Table 4 and Fig. 5.

DISCUSSION

According to literature data [Giterman, 1963; Tomskaya, 1981; Ivanov, 1984; Fotiev, 2006], the IC in Central Yakutia began to accumulate in the Murukhtin interval (MIS 4), but the most favorable climatic conditions for the accumulation of loesslike sediments with ice wedges occurred in the Kargin epoch of the Late Pleistocene (MIS 3). Sediments of this age contain a large number of the remains of mammoth fauna and steppe and tundra-steppe vegetation with a subordinate role of tree species.

Accumulation of sediments continued throughout the second half of the Late Pleistocene and ended at the end of the Sartan epoch [Ivanov, 1984]. The climate was rather severe and sharply continental; the mean annual temperature of permafrost in Central Yakutia, where the ice complex was formed, did not exceed -10°C [Konishchev, 1997, 2011].

In MIS 3, the role of steppe communities grew due to increasing continentality and decreasing pre-

cipitation. The main associations of cold steppes were grassy and forb-wormwood groups with predominance of xerophytes. Steppe areas alternated with small areas of larch woodland with an admixture of *Betula alba* and shrubs. Groves of *Pinus pumila* and *P. sylvestris* were found in drier areas on drained watersheds and terrace edges [Giterman, 1963; Shofman et al., 1977; Tomskaya, 1981; Fotiev, 2006]. The role of tree species increased during more favorable periods of MIS 3 in Central Yakutia [Tomskaya, 1981].

In the Sartan epoch, the continentality of the climate increased compared to that in the Kargin epoch; a decrease in precipitation, climate drying, aggradation of permafrost, and growth of wedge ice in the IC sediments took place [Galanin, 2021]. Forest areas reduced in size, whereas areas under wormwood-grass-forb communities increased. There were also birch and larch woodlands with steppe vegetation in the ground cover and thickets of dwarf birch species [Andreev et al., 2002], as well as unfixed bare sands and stony deserts [Pavlova et al., 2017; Galanin, 2021].

According to the results of the present study, the IC within the strath terrace of the Vilyui River in its lower course was formed from the end of the Kargin epoch to the first half of the Sartan epoch. According to A.A. Galanin [Galanin et al., 2019], the formation of the IC sediments studied in 2016 (section 489) dates to MIS 2 and the beginning of the Holocene. Spore-pollen spectra obtained from section 489 (interval 4.7–0.3 m) indicate very dry and cold climatic conditions and relatively poor vegetation cover of the surrounding landscapes. During that period, open-

type landscapes – cold dry steppes with a predominance of xerophytic communities (Poaceae, Caryophyllaceae, *Artemisia*, Brassicaceae), in some places mixed forb-grass meadows and nearly barren sandy spaces – were widespread. Low concentrations of pollen and the presence of spores of coprophilous *Glomus* fungi in large numbers in the PZI palynozone are typical of eolian landscapes [Aptroot, van Geel, 2006; Graf, Chmura, 2006; Chambers et al., 2010] and indicate the dry conditions of sedimentation and high intensity of soil erosion. In some places, larch woodlands and thickets of dwarf birch, alder, and willow were formed.

Sediments exposed in section 489 in the interval of 0.1–5 m are represented by loamy sands and silty sands; their palynological analysis confirms the fact of the unfavorable conditions for the vegetation development (pollen concentration in general throughout the sediment pack varies from 0 to 293 grains/cm³). However, according to the obtained data, within this interval, there are variations that allow us to distinguish the unfavorable and more favorable periods of the sediment formation and the vegetation cover development. In the interval of 5–4.5 m, where the transitional pack from the Diolkuma Formation to the IC and the base of the IC occur, the pollen is almost absent or very low (Fig. 4); it ranges from 0 to 22 grains/cm³, and the I_r content is 0.14–0.35%. The time of the sediment formation falls on the cold stage at the end of the Kargin epoch.

In the interval of 4.5–2.8 m, the loamy sandy sediments are saturated with organic detritus and remains of herbaceous plants; the concentration of pollen sharply increases (67–293 grains/cm³), as well as the organic matter content ($I_r = 3.89–7.59\%$). Presumably, the formation of this sediment member dates to the end of the Kargin epoch – the beginning of the Sartan epoch, when a slight warming took place and conditions were favorable to contribute to greater productivity of the vegetation cover.

In the interval of 2.8–1.4 m the loamy sandy sediments display a decrease in the contents of pollen and I_r from the bottom to the top of the section from 51 to 12 grains/cm³ and from 1.63 to 1.36%, respectively. This was the period of colder climate, which contributed to a decrease in plant productivity. Presumably, this period corresponds to the first half of the Sartan epoch.

The accumulation of sediments in the interval of 1.4–0.1 m could take place during the Last Glacial Maximum (LGM, ~26 to 19 ka BP according to [Cohen, Gibbard, 2019]), probably, it could have continued up to the present time. In the period from the LGM to the beginning of the Holocene, the climatic conditions in Central Yakutia reached an exceptionally critical level. This led to the significant degradation of not only woody vegetation but also cold steppes and the expansion of the areas of sand barrens

and dune massifs of the Diolkuma Formation [Galanin, Pavlova, 2019]. In the Holocene, this member was affected by various processes during thawing and freezing of sediments. This contributed to the development of cryoturbation. Because of cryoturbation, the MPI-97 date (¹⁴C) obtained for a sample from the depth of 0.5 m from the surface turned out to be less than 100 years. The pollen content is 59 grains/cm³, and the I_r content is 2.97%, indicating a possible increase in plant productivity during the Late Holocene.

Chemical and isotopic composition of ice wedges

Ice wedges of moderately fresh composition with a relatively narrow range of changes in mineralization and trace element concentrations, with a predominance of HCO₃⁻ and Ca²⁺ ions were formed within the Kargin–Sartan syncryogenic sediment sequence, generally due to atmospheric precipitation (in particular, snowmelt water) entering frost cracks.

The ice samples have a rather high content of Fe, Al, Sr, Ba, Mn, Br, Ti, Cu, B, V and Ni. As it is known, within the permafrost zone, under the conditions of freezing shallow lakes and bogs in most cases, iron and manganese hydroxides are precipitated; their mobility is determined by redox and acid–base conditions. In the reducing gley medium with acid reaction, these elements are mobile and migrate in soluble form. Under the oxidizing conditions, or reducing hydrogen sulfide conditions these elements are precipitated upon an increase in pH [Makarov, 1985]. The increased content of iron and manganese, as well as other heavy elements, such as vanadium, cobalt, and strontium, in the studied wedge ice indicates an acid gley medium during the wedge ice formation and confirms a minor contribution of water from shallow freezing lakes and bogs confined to microrelief depressions that formed on the top of the IC. A number of studies of wedge ice in Yamal and northern Yakutia link an increased content of heavy metals in the ice with the participation of bog waters [Budantseva, Vasil'chuk, 2017; Vasil'chuk et al., 2017]. According to the analysis of the ratio of anions and cations in the investigated ice samples, the ice wedge was formed from waters of the second and third types according to the classification of O.A. Alekin [1975]. The obtained data show that low-mineralized suprapermafrost waters associated with washing of the underlying quartz-feldspar rocks could have taken a small part in the ice formation. The Na/Cl coefficient in all the studied samples is less than 1, which indicates that waters of different degrees of metamorphization have been involved in the formation of the ice wedge.

A comparison of the chemical composition of ice wedge with the composition of modern surface and groundwater (lakes, the Vilyui River and its tributaries, springs confined to massifs of dune sands) sam-

Table 5. Average concentrations of the main trace elements in ice wedges, different types of modern waters in the lower reaches of the Vilyui River and in global river water (river water clarke)

Element, $\mu\text{g/L}$	Ice wedges ($n = 16$)	Type of natural waters						River water clarke [Solovov <i>et al.</i> , 1990]
		Vilyui River ($n = 2$)	Rainwater ($n = 2$)	Intrapermafrost waters		Lake waters		
				Kysyl-Syr Tukulan ($n = 11$)	Makhatta Tukulan ($n = 2$)	Interdune lakes ($n = 10$)	Oxbow lakes ($n = 2$)	
B	4.9	7.0	0.9	2.1	5.2	4.4	4.3	20
Al	534.3	27.8	13.4	517.2	127.8	5.2	3.0	160
Ti	14.0	0.6	0.0	9.1	2.4	0.1	0.0	3
V	4.3	0.9	0.0	7.4	0.9	0.0	0.3	1
Cr	1.3	0.0	0.0	1.1	0.0	0.0	0.0	1
Mn	34.1	16.3	8.9	759.4	74.5	25.7	58.6	10
Fe	1650.6	146.6	27.5	6391.8	1517.5	179.6	492.2	40
Co	0.6	0.1	0.0	10.1	0.4	0.0	0.0	0.3
Ni	3.1	1.5	0.0	6.2	0.9	0.1	0.2	2.5
Cu	5.0	1.7	3.7	3.2	0.7	0.1	0.2	7
Zn	2.7	3.7	6.4	7.9	1.7	1.6	1.2	20
As	0.3	0.4	0.0	2.5	0.6	0.2	1.2	2
Br	29.5	26.3	0.0	0.0	0.0	7.2	10.2	20
Sr	77.3	88.5	7.4	39.8	74.9	49.3	51.2	50
Ba	34.9	12.7	8.3	53.4	25.6	31.3	21.3	30
Pb	0.6	0.1	0.1	3.5	0.3	0.0	2.3	1

pled during field studies (Table 5), as well as literature data [Shepelev, 1981; Pavlova *et al.*, 2022; Palamarchuk *et al.*, 2023], indicates that the considered region is characterized by the increased content of iron, manganese, aluminum, strontium, and barium compared to the average chemical composition of groundwater in the permafrost zone. The source of iron is feldspars, the content of which in the underlying eolian cover sands is up to 21–25%, as well as aluminosilicate minerals of heavy fraction (hornblende, epidote, ilmenite, staurolite) [Galanin *et al.*, 2018].

The dissolved form of iron appears under the influence of organic acids, carbon dioxide, etc. The presence of organic matter in intrapermafrost waters of the Makhatta Tukulan is indirectly indicated by their high oxidizability. Increased concentrations of manganese, strontium, and barium are noted in surface and ground waters due to the presence of organic acids. The presence of acids in water contributes to the mobilization and migration of these elements, as well as to their rapid accumulation. The analysis of the isotopic compositions of two relatively closely located ice wedges indicates that they were formed in different time intervals of the Late Pleistocene. Thus, according to the obtained data, syngenetic ice wedge, sampled on the strath terrace of the Vilyui River in 2021 (section 052) has a relatively light isotopic composition: $\delta^{18}\text{O} = -(29.2 \pm 0.3)\text{‰}$, $\delta\text{D} = -(226.6 \pm \pm 2.3)\text{‰}$, $d_{\text{exc}} = (6.8 \pm 0.5)\text{‰}$. These values attest to an insignificant variation of the isotopic composition within ice wedge. The deuterium excess in most samples is less than 8, indicating little influence of fractionation processes on the primary isotopic signal of

the water source (Fig. 6). The regression equation has the following form: $\delta\text{D} = 7.11\delta^{18}\text{O} + 19.25$ ($R^2 = 0.97$); it is very similar to the equation for precipitation of the cold season in Yakutsk: $\delta\text{D} = 8.17\delta^{18}\text{O} + 21.9$; $R^2 = 0.99$ [Papina *et al.*, 2017]. The slope of the $\delta\text{D}/\delta^{18}\text{O}$ ratio line (the value is 7.11) and the deuterium excess (6.8 ± 0.5) demonstrate that atmospheric precipitation (snowmelt water) was the main source of the ice formation, and it was subjected to relatively weak isotopic transformation (during evaporation and sublimation) under the conditions of lower temperatures and thinner snow cover (in comparison with those at present).

The wedge uncovered in 2016 (section 489) has a heavier isotopic composition ($\delta^{18}\text{O} = -(27.2 \pm 1.4)\text{‰}$, $\delta\text{D} = -(215.8 \pm 8.5)\text{‰}$, $d_{\text{exc}} = (1.7 \pm 3.1)\text{‰}$) with a higher variability compared to the ice wedge from section 052 [Galanin *et al.*, 2019]. The deuterium excess in four samples out of six is negative (Fig. 6). This points to the significant influence of fractionation processes on the primary isotopic signal of snowmelt water, or to the fact that meltwater had been highly depleted in heavy isotopes when initially entering the frost crack. The regression equation is as follows: $\delta\text{D} = 5.92\delta^{18}\text{O} - 54.76$ ($R^2 = 0.99$). It radically differs by very low angular coefficients from the equation characterizing modern precipitation of the cold season in Yakutsk and from the equation characterizing local meteoric water line in Yakutsk ($\delta\text{D} = 7.81\delta^{18}\text{O} - 1.57$; $R^2 = 0.99$) [Galanin *et al.*, 2019]. The isotopic compositions of the spring snow stock ($\delta\text{D} = 6.85\delta^{18}\text{O} - 31.88$; $R^2 = 0.99$) are the closest modern analogues

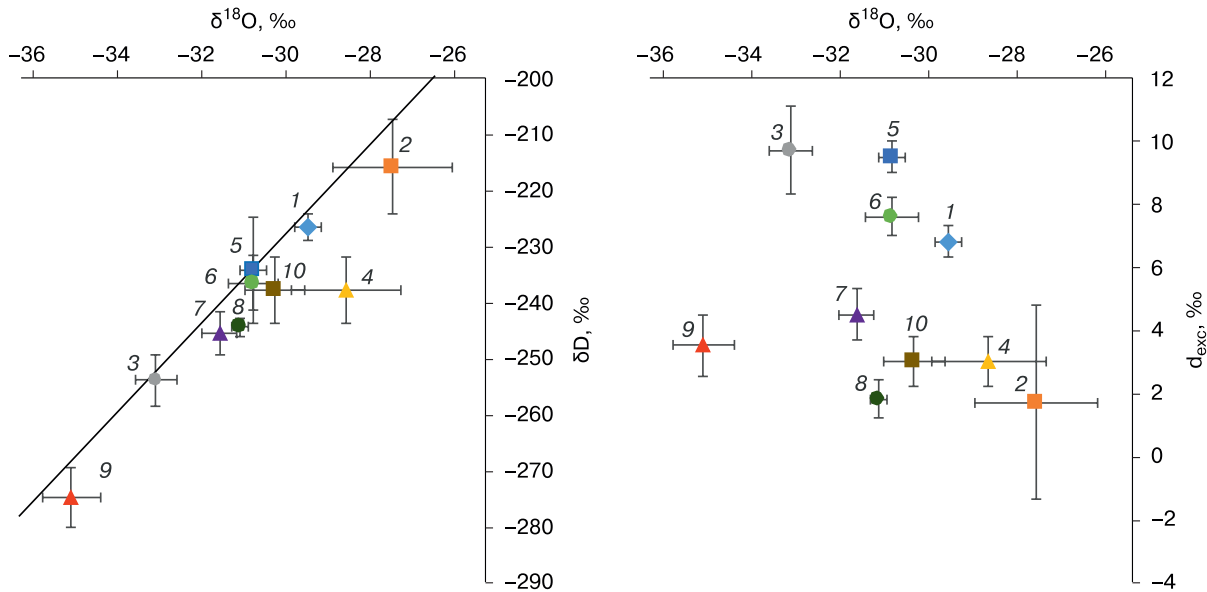


Fig. 6. Mean values of $\delta^{18}\text{O}/\delta\text{D}$ and d_{exc} of ice wedges of differently elevated terraces of the Central Yakutian Plain in MIS 4–2:

1 – strath terrace of the Vilyui River, section 052 (2021), MIS 3–2; 2 – strath terrace of the Vilyui River, section 489 (2016), MIS 3–2 [Galanin et al., 2019]; 3 – Tyalycham outcrop, Vilyui River, MIS 4–3 [Galanin et al., 2019]; 4 – Khomustakh outcrop, Verkhnevilyuisk, MIS 3–2 (authors' data); 5 – Tanda outcrop, Tanda River, MIS 3 [Opel et al., 2019]; 6 – Mamontova Gora, the Aldan River, MIS 3–2; 7 – Ulakhan–Syrdakh, Lena–Amga interfluve, MIS 2; 8 – Lake Syrdakh, Lena–Amga interfluve, MIS 2 [Popp et al., 2006]; 9 – Tit-Ary-1, 10 – Tit-Ary-2 outcrops, Prilenskoe Plateau, MIS 4–3 [Galanin et al., 2019].

of the studied ice wedge, which indicates drier conditions of the Sartan epoch compared to the Kargin epoch of the Late Pleistocene, as well as the low thickness of the snow cover and extremely insufficient moisture availability in the cryogenic landscapes of Central Yakutia [Galanin et al., 2019].

In Central Yakutia, syngenetic ice wedges are widespread. The isotopic composition of the ice has the greatest similarity to the isotopic composition of atmospheric precipitation of the winter season. According to previous investigations [Popp et al., 2006; Galanin et al., 2019; Opel et al., 2019], ice wedges, formed in the first half of the Late Pleistocene (MIS 4–MIS 3), for example, in Tit-Ary-1, Tit-Ary-2, and Tyalycham outcrops, have the lightest isotopic composition (Fig. 6). Ice wedges formed in MIS 3–MIS 2 have a heavier isotopic composition, while younger wedges attributed to the Sartan epoch (MIS 2) (e.g., ice wedges sampled in 2016 in section 489) have the heaviest isotopic composition with clear signs of evaporative fractionation. The obtained sequence shows that there was a gradual increase in continentality and drying of the climate starting from MIS 4. Further, during MIS 3 and the Sartan epoch (MIS 2), the aridization of the climate in Central Yakutia reached its maximum, which was manifested in a decrease in the annual precipitation and in the snow cover thickness, an increase in the role of winter

evaporation, and a heavier isotopic composition of snow by the beginning of the snowmelt season. This is probably the reason why, despite the colder climatic conditions of MIS 2 compared to the previous epoch, ice wedges of this age have a heavier isotopic composition [Galanin et al., 2019].

CONCLUSIONS

1. The ice complex studied on the strath terrace of the Vilyui River valley in its lower course was formed from the end of the Kargin epoch and throughout the Sartan epoch under very dry and cold conditions, when open-type landscapes of dry cold steppes with a predominance of xerophytic communities, in some places, mixed forb-grass meadows, as well as almost unvegetated sandy areas were widespread, alternating with larch woodlands and thickets of dwarf birch, alder, and willow species.

2. Low mineralization (0.07–0.29 g/dm³) with a predominance of calcium bicarbonate in ice samples indicates that the main source of the ice wedges formation was winter precipitation – snowmelt water. Relatively high content of heavy metals (iron, manganese, vanadium, strontium, cobalt) in the studied ice samples suggests an acidic gley medium during the ice wedges formation and a possible small participation of water of shallow freezing lakes and bogs confined to the polygonal relief hollows. At the same

time, according to the obtained data, suprapermfrost waters of low mineralization were involved in the ice wedges formation.

3. The ice wedges in the upper part of the studied strath terrace have a relatively light isotopic composition, which is very similar to cold-season precipitation in Yakutsk (for the ice wedge from section 052) and spring snow stock (for the ice wedge from section 489). The obtained data indicate arid conditions, low snow cover thickness, and strong moisture deficit in the cryogenic landscapes of Central Yakutia. The deuterium excess indicates that evaporative processes prevailed during the ice formation. Analysis of the obtained isotopic compositions of two relatively adjacent ice wedges indicates that they were formed in different time intervals of the Late Pleistocene.

Acknowledgments. *The authors are grateful to I.V. Klimova, G.I. Shaposhnikov, O.V. Shepeleva, and L.Yu. Boitsova of the Melnikov Permafrost Institute, Siberian Branch of the Russian Academy of Sciences for assistance in analytical work.*

The study was performed within the framework of state assignment no. 122011800064-9 "Structure and Key Stages of the Evolution of the Continental Cryolithozone in the Neopleistocene and Holocene".

References

- Alekin O.A., 1975. *The Basics of Hydrochemistry*. Leningrad, Gidrometeoizdat, 296 p. (in Russian)
- Alekseev M.N., 1961. *Stratigraphy of Continental Neogene and Quaternary Deposits of the Vilyui Depression and the Lena River Valley in the Lower Reaches*. Moscow, Izd. Akad. Nauk SSSR, 120 p. (in Russian)
- Alekseev M.N., Kuprina N.P., Medyantsev A.I. et al., 1962. *Stratigraphy and Correlation of Neogene and Quaternary Deposits in the Northeastern Part of the Siberian Platform and Its Eastern Folded Framing*. Moscow, Izd. Akad. Nauk SSSR, 127 p. (in Russian)
- Andreev A.A., Klimanov V.A., Sylerzhitskii L.D., 2002. History of vegetation and climate of Central Yakutia in the Late Glacial and Holocene. *Bot. Zh.* 7, 86–98. (in Russian)
- Aptroot A., van Geel B., 2006. Fungi of the colon of the Yukagir Mammoth and from stratigraphically related permafrost sample. *Rev. Palaeobot. Palynol.* 141, 225–230.
- Bronk R.C., 2009. Bayesian analysis of radiocarbon dates. *Radiocarbon* 51 (1), 337–360.
- Budantseva H.A., Vasil'chuk Yu.K., 2017. Geochemical composition of Holocene ice wedge of Southern and Central Yamal Peninsula. *Arktika Antarktika* 1, 1–22. (in Russian)
- Chambers F.M., van Geel B., van der Linden M., 2010. Considerations for the preparation of peat samples for palynology, and for the counting of pollen and non-pollen palynomorphs. *Mires Peat* 7 (11), 1–14.
- Cohen K.M., Gibbard P.L., 2019. Global chronostratigraphical correlation table for the last 2.7 million years, version QI9 QI-500. *Quat. Int.* 500, 20–31.
- Danilov N.S. (Ed.), 2005. *Diversity of the Flora of Yakutia*. Novosibirsk, Izd. Sib. Otd. Ross. Akad. Nauk, 326 p. (in Russian)
- Ershov E.D. (Ed.), 1989. *Geocryology of the USSR. Central Siberia*. Moscow, Nedra, 413 p. (in Russian)
- Faegri K., Iversen J., 1989. *Textbook of Pollen Analysis*. UK, Chichester, J. Wiley & Sons, 328 p.
- Fotiev S.M., 2006. Modern conceptions of the evolution of cryogenic area of Western and Eastern Siberia in Pleistocene and Holocene (report 2). *Kriosfera Zemli* X (2), 3–26. (in Russian)
- Galanin A.A., 2021. Late Quaternary sand covers of Central Yakutia (Eastern Siberia): structure, facies composition and paleoenvironment significance. *Earth's Cryosphere XXV* (1), 3–30.
- Galanin A.A., Pavlova M.R., 2019. Late Quaternary dune formations (D'olkuminskaya series) in Central Yakutia (part 2). *Earth's Cryosphere XXIII* (1), 3–15.
- Galanin A.A., Pavlova M.R., Klimova I.M., 2018. Late Quaternary dune formations (D'olkuminskaya series) in Central Yakutia (part 1). *Earth's Cryosphere XXII* (6), 3–14.
- Galanin A.A., Pavlova M.R., Papina T.S. et al., 2019. Stable isotopes of ^{18}O and D in key components of water flows and permafrost in Central Yakutia (Eastern Siberia). *Led Sneg* 59 (3), 333–354. (in Russian)
- Gavrilova M.K., 1973. *The Climate of Central Yakutia*. Yakutsk, Yakutsk. Kn. Izd., 119 p. (in Russian)
- Giterman R.E., 1963. *Stages of the Development of Quaternary Vegetation in Yakutia and Their Significance for Stratigraphy*. Moscow, Akad. Nauk SSSR, 191 p. (in Russian)
- GOST (State Standard) 12536-2014, 2015. *Soils. Methods for Laboratory Determination of Granulometric (Grain-Size) and Microaggregate Composition*. Moscow, Standartinform, 22 p. (in Russian)
- GOST (State Standard) 23740-2016, 2017. *Soils. Methods for Determining the Content of Organic Substances*. Moscow, Standartinform, 12 p. (in Russian)
- Graf M.T., Chmura G.L., 2006. Development of modern analogues for natural, mowed and grazed grasslands using pollen assemblages and coprophilous fungi. *Rev. Palaeobot. Palynol.* 141, 139–149.
- Grimm E., 2004. *Tilia software 2.0.2*. USA, Illinois State Museum Research and Collection Center, Springfield, 2004.
- Gromov V.I., 1948. *Paleontological and Archaeological Substantiation of the Stratigraphy of Continental Quaternary Deposits on the Territory of the USSR (Mammals, Paleolithic)*. Moscow, Izd. Akad. Nauk SSSR, 524 p. (in Russian)
- Hoefs J., 1997. *Stable Isotope Geochemistry*. Berlin, Germany, Springer Verlag, 201 p.
- Ivanov M.S., 1984. *Cryogenic Structure of the Quaternary Deposits of the Lena–Aldan Depression*. Novosibirsk, Nauka, 125 p. (in Russian)
- Katasonov E.M., Ivanov M.S., 1973. *Cryolithology of Central Yakutia (Excursion to Lena and Aldan): Guidebook*. Yakutsk, Izd. OUPES Sib. Otd. Akad. Nauk SSSR, 37 p. (in Russian)
- Katasonova E.G., Tolstov A.N., 1963. Geocryological features of windblown sands (tukulans) on the right bank of the Vilyui River. In: *Permafrost in Different Regions of the USSR*. Moscow, Izd. Akad. Nauk SSSR, p. 166–178. (in Russian)
- Konishchev V.N., 1997. Cryolithogenic method of the assessment of paleotemperature conditions of formation of the ice complex and subaerial periglacial sediments. *Kriosfera Zemli* I (2), 23–28. (in Russian)
- Konishchev V.N., 2011. Permafrost response to climate warming. *Earth's Cryosphere XV* (4), 13–16.
- Makarov V.N. (Ed.), 1985. *Migration of Chemical Elements in the Cryolithozone*. Novosibirsk, Nauka, 129 p. (in Russian)

- Meyer H., Dereviagin A.Y., Siegert C. et al., 2002. Palaeoclimate reconstruction on Big Lyakhovsky Island, North Siberia – hydrogen and oxygen isotopes in ice wedges. *Permafr. Periglac. Process.* **13** (2), 91–105.
- Meyer H., Opel T., Laepple T. et al., 2015. Long-term winter warming trend in the Siberian Arctic during the mid-to late Holocene. *Nature Geosci.* **8** (2), 122–125.
- Opel T., Murton J. B., Wetterich S. et al., 2019. Past climate and continentality inferred from ice wedges at Batagay megaslump in the Northern Hemisphere's most continental region, Yana Highlands, interior Yakutia. *Clim. Past.* **15** (4), 143–146.
- Palamarchuk V.A., Lebedeva L.S., Pavlova N.A. et al., 2023. Current state of the groundwater springs of the Mahatta sand massif, Eastern Siberia. *Earth's Cryosphere XXVII* (4), 21–32.
- Papina T.S., Malygina N.S., Eirikh A.N. et al., 2017. Isotopic composition and sources of atmospheric precipitation in Central Yakutia. *Earth's Cryosphere XXI* (2), 52–61.
- Pavlova M.R., 2018. Lithofacies characteristics of deposits of the 65-m-high strath terrace of the Vilyui River (Central Yakutia). In: Materials of the XI Int. Sci. Pract. Conf. of Students, Postgraduates and Young Scientists *Geology in the Developing World* (Perm', April 10–13, 2018). Perm', vol. 2, p. 280–283. (in Russian)
- Pavlova M.R., Rudaya N.A., Galanin A.A. et al., 2017. Structure and evolution of dune massifs in the Vilyui River basin over the Late Quaternary period (by the example of the Makhatta and Kysyl-Syr Tukulan). *Contemp. Probl. Ecol.* **10** (4), 411–422.
- Pavlova N.A., Lebedeva L.N., Baishev N.E. et al., 2022. Geochemistry of surface and groundwater of tukulan Makhatta (Central Yakutia). In: Materials of the XII All-Russia Sci. Pract. Conf. *Geology and Mineral Resources of the Northeast of Russia* (Yakutsk, March 23–25, 2022). Yakutsk, Izd. Sev-Vost. Fed. Univ., p. 440–445. (in Russian)
- Pokrovskaya I.M. (Ed.), 1950. *Pollen Analysis*. Moscow, Gosgeolizdat, 570 p. (in Russian)
- Popp S., Diekmann B., Meyer H. et al., 2006. Paleoclimate signals as inferred from stable-isotope composition of ground ice in the Verkhoyansk foreland, Central Yakutia. *Permafr. Periglac. Process.* **17**, 119–132.
- Reimer P.J., Austin W.E.N., Bard E. et al., 2020. The IntCal20 Northern Hemisphere radiocarbon age calibration Curve (0–55 cal BP). *Radiocarbon* **62** (4), 1–33.
- Romanovsky N.N., 1993. *Basics of Cryogenesis of the Lithosphere*. Moscow, Izd. Mosk. Gos. Univ., 366 p. (in Russian)
- Sakharova M.S., Cherkasov Yu.A., 1970. *Immersion Method of Mineralogical Study*. Moscow, Izd. Mosk. Gos. Univ., 89 p. (in Russian)
- Schirrmeister L., Dietze E., Matthes H. et al., 2020. The genesis of Yedoma Ice Complex permafrost – grain-size end member modeling analysis from Siberia and Alaska. *Quat. Sci. J.* **69**, 33–53.
- Schirrmeister L., Fedorov A.N., Froese D. et al., 2022. Editorial: Yedoma permafrost landscapes as past archives, present and future change areas. *Frontiers Earth Sci.* **10**, 6–10.
- Schirrmeister L., Froese D., Tumskey V. et al., 2013. Yedoma: Late Pleistocene Ice-Rich Syngenetic Permafrost of Beringia. In: *Encyclopedia of Quaternary Science*. Netherlands, Amsterdam, Elsevier, p. 542–552.
- Shaposhnikov G.I., Galanin A.A., Lytkin V.M. et al., 2019. Absolute dates obtained in 2015–2017 by the radiocarbon laboratory of Melnikov Permafrost Institute (Siberian Branch of the Russian Academy of Sciences). *Prirodn. Res. Arktiki Subarkтики* **24** (3), 39–49. (in Russian)
- Shepelev V.V., 1981. Groundwater of tukulans of Central Yakutia. In: *Aeolian Formations of Central Yakutia*. Yakutsk, Inst. Merzlotoved. Sib. Otd. Akad. Nauk SSSR, p. 30–41. (in Russian)
- Shofman I.L., Kind N.V., Paxomov M.M. et al., 1977. New data on the age of low terraces in the Vilyui River basin. *Buyl. Komiss. Izuchen. Chetvertichn. Perioda* (Moscow), **47**, 64–69. (in Russian)
- Shvartsev S.L., 1996. *General Hydrogeology*. Moscow, Nedra, 424 p. (in Russian)
- Soloviev P.A., 1959. *Cryolithozone of the Northern Part of the Lena–Amga Interfluve*. Moscow, Izd. Akad. Nauk SSSR, 144 p. (in Russian)
- Solovov A.P., Arkhipov A.Ya., Bugrov V.A. (Eds.), 1990. *Handbook of Geochemical Prospecting for Minerals*. Moscow, Nedra, 335 p. (in Russian)
- Tomskaya A.I., 1981. *Palynology of the Cenozoic of Yakutia*. Novosibirsk, Nauka, 224 p. (in Russian)
- Vasil'chuk Yu.K., Budantseva N.A., Vasil'chuk D.Yu., 2017. Heavy metals and trace elements in the Late Pleistocene ice wedge of Northern Yakutia. *Arktika Antarktika* **1**, 23–37. (in Russian)

Received May 8, 2024

Revised August 1, 2024

Accepted October 19, 2024

Translated by V.A. Krutikova